



Published in final edited form as:

*J Am Chem Soc.* 2010 July 14; 132(27): 9335–9340. doi:10.1021/ja1009162.

## Origins of Stereoselectivity in the *trans*-Diels-Alder Paradigm

Robert S. Paton<sup>1</sup>, Joel L. Mackey<sup>1</sup>, Woo Han Kim<sup>2</sup>, Jun Hee Lee<sup>3</sup>, Samuel J. Danishefsky<sup>2,3</sup>, and K. N. Houk<sup>1,\*</sup>

<sup>1</sup> Department of Chemistry and Biochemistry, University of California, Los Angeles, 607 Charles E. Young Drive, Los Angeles, California 90095-1569

<sup>2</sup> Laboratory for Bioorganic Chemistry, Sloan-Kettering Institute for Cancer Research, 1275 York Avenue, New York, New York 10065

<sup>3</sup> Department of Chemistry, Columbia University, Havemeyer Hall, 3000 Broadway, New York, New York 10027

### Abstract

The regioselectivity and stereoselectivity aspects of the Diels-Alder/radical hydrodenitration reaction sequence leading to *trans*-fused ring systems have been investigated with density functional calculations. A continuum of transition structures representing Diels-Alder and hetero-Diels-Alder cycloadditions as well as a sigmatropic rearrangement have been located, and they all lie very close in energy on the potential energy surface. All three pathways are found to be important in the formation of the Diels-Alder adduct. Reported regioselectivities are reproduced by the calculations. The stereoselectivity of radical hydrodenitration of the *cis*-Diels-Alder adduct is found to be related to the relative conformational stabilities of bicyclic radical intermediates. Overall, the computations provide understanding of the regioselectivities and stereoselectivities of the *trans*-Diels-Alder paradigm.

### Introduction

The critical role of the Diels-Alder reaction in organic synthesis is well appreciated. Diels-Alder cycloadditions produce *cis*-fused bicyclic systems from cyclic *cis*-dienophiles, providing a routine approach to the synthesis of complex molecules. Danishefsky and co-workers recently reported a departure from the *cis*-directed logic of the traditional Diels-Alder approach to encompass the formation of *trans*-fused products (i.e. the *trans* Diels-Alder paradigm).<sup>1</sup> This process formally involves reactions leading formally to the *trans*-fused adduct of a cycloalkene. This was achieved not via antarafacial cycloaddition, but instead by equipping an otherwise unreactive dienophile (such as cyclohexene) with a temporary, readily removable activating group. Following cycloaddition, the resultant *cis*-fused substructure is converted to the *trans*-series by removing the activating group and replacing it in a stereocontrolled fashion (Scheme 1).

The nitro group was chosen, based on its dienophile activating properties, its known success in controlling Diels-Alder (DA) regioselectivity, and its ability to generate free radical intermediates. DA cycloadducts were obtained for the reaction between 1-nitrocyclohexene and a series of hydrocarbon dienes, although yields were adversely affected by the

houk@chem.ucla.edu.

Supporting Information Available

Absolute energies, Cartesian coordinates, imaginary frequencies, and full authorship of reference <sup>25</sup>. This material is available free of charge via the Internet at <http://pubs.acs.org>

decomposition of 1-nitrocyclohexene. Alcoholic solvents, especially 2,2,2-trifluoroethanol, were found to improve yields of cycloaddition, and microwave irradiation was also helpful (Scheme 2).

Nitroalkenes can function as either dienophiles or as *hetero-dienes* in Diels-Alder reactions (Scheme 3).<sup>2</sup> Denmark has shown that the reactions of nitroalkenes with cyclopentadiene can lead to mixtures of DA and hetero-Diels-Alder (HDA) cycloadducts.<sup>3–8</sup> The DA adduct is favored under thermal conditions, but a Lewis acid can reverse the periselectivity to favor the HDA adduct. Calculations reveal that under thermal conditions this reaction proceeds initially via an *endo* DA transition state, which is then followed by a sigmatropic rearrangement of the *endo* adduct accounting for the formation of the hetero-Diels-Alder cycloadduct.<sup>9</sup> Diels-Alder reactions of nitroethylene derivatives with cyclohexadiene yield a mixture of DA and HDA adducts. Subsequently the HDA adduct rearranges to the DA adduct upon heating at 80 °C via a [3,3] sigmatropic rearrangement.<sup>10</sup> Computational studies on microwave-assisted reactions of nitroheterocycles with dienes suggest that the DA adduct is formed via a tandem HDA/[3,3]-sigmatropic shift.<sup>11</sup>

When reactants pass through an initial transition state into a flat area of an energy surface with multiple exit routes to products, reaction dynamics affect the selectivity. The products that tend to form, arise from a direct continuation of the trajectories that passed through the initial transition state.<sup>12–14</sup> In such cases, dynamics determine the selectivity in cases involving a bifurcating energy surface. Theoretical studies by Caramella showed that the dimerization of cyclopentadiene involves a bifurcating energy surface, and a transition state that is “bispericyclic”.<sup>15</sup> Singleton has discussed the role of bifurcating energy surfaces in cycloadditions where there are competing [4+2] and [2+4] pathways.<sup>16</sup> Bifurcating energy surfaces have now been implicated in determining the selectivity of a variety of Diels-Alder reactions.<sup>17–21</sup>

The removal of the activating nitro group was achieved by radical hydrodenitration, using tri-*n*-butyltin hydride and AIBN. The mechanism of this transformation presumably proceeds via trialkyltin radicals forming a Sn-O bond with the nitro group. Fragmentation gives rise to Bu<sub>3</sub>SnONO and a (secondary or tertiary) alkyl radical.<sup>22</sup> This transformation has been used successfully to reduce the nitro group of Diels-Alder cycloadducts.<sup>23,24</sup> In Danishefsky's recent work, the *cis*-fused ring junction characteristic of the Diels-Alder cycloaddition was converted to the desired *trans* stereochemistry for the decalins shown in Scheme 4. Radical hydrodenitration of 6,6-bicyclics formed from cycloaddition of nitrocyclohexene yielded the *trans* stereochemistry selectively, although 5,6-bicyclics from the cycloadditions of nitrocyclopentene showed very little selectivity.

In order to understand the factors that control the regioselectivity of the cycloaddition, and how the *trans*-fused decalin geometry is ultimately furnished from the *cis*-fused cycloadduct, a computational study using density functional theory (DFT) calculations was undertaken.

## Computational Methods

All geometry optimizations were performed with Gaussian 09 using the B3LYP density functional with the 6-31G(d) basis set.<sup>25</sup> A fine grid density was used for numerical integration. Radical species were optimized with unrestricted (UB3LYP) density functional calculations. We have shown previously that this level of electronic structure theory is capable of providing ground-state and transition-state geometries for organic radicals that agree well with more elaborate calculations, and that the results obtained agree quantitatively with experiment.<sup>26</sup> We have also performed single point energy calculations

with M06-2X/UM06-2X density functional theory (DFT)<sup>27</sup> that are expected to deliver a more accurate treatment of medium-range correlation effects, such as van der Waals interactions. Such calculations give improved thermodynamics for C-C bond forming reactions.<sup>28</sup> Energetics were also evaluated with the B2-PLYP double-hybrid density functional,<sup>29</sup> again to ensure that our conclusions are robust across different theoretical methods. Single point calculations with a larger 6-311+G(d,p) basis set have been also performed to confirm that the basis-set size does not affect the conclusions drawn. Harmonic vibrational frequencies were computed for all optimized structures in order to verify that they were either minima (zero imaginary frequencies) or transition states (a single imaginary frequency). Zero-point energies (unscaled) are included in all thermodynamic quantities. The effects of solvation on the reaction energetics were evaluated using a conductor-like polarizable continuum solvation model (CPCM).<sup>30</sup> The solute surface was defined by UAKS radii in each case.<sup>31</sup>

## Results and Discussion

The cycloaddition between 2,3-dimethyl-1,3-butadiene and 1-nitrocyclohexene was investigated, and transition structures (TSs) for both the Diels-Alder (1-nitrocyclohexene behaving as dienophile) and the hetero-Diels-Alder (1-nitrocyclohexene behaving as *heterodiene*) reactions were successfully located, as shown in Figure 1. The activation barriers for the competing DA and HDA mechanistic pathways are very similar at all of the levels of theory examined, so both mechanisms are predicted to be competitive (see Supporting Information for a full comparison of energetics computed with different methods). The HDA TS with an isopropenyl group *endo* to the hetero-diene is most favored by 1.1 kcal/mol. With the inclusion of solvation effects, the preference for the HDA TS rises to 1.5 kcal/mol. TSs for the regioisomeric HDA pathway were located (see Supporting Information) but lie around 10 kcal/mol higher in energy than those shown in Figure 1, and so can be discounted as a viable pathway. While the kinetics of DA and HDA pathways are predicted to be very similar, there is a large difference in the thermodynamics of the two processes; the DA adduct is over 18 kcal/mol more stable than the HDA adduct. B3LYP is expected to underestimate the exothermicity of the Diels-Alder reaction, due to a systematic error in computing  $\pi$ - $\sigma$  energy changes. M06-2X calculated energetics, which are expected to be more accurate, predict that reactions are more exothermic than predicted by B3LYP as is found in other Diels-Alder processes.<sup>28</sup> However, the DA adduct is still much preferred over the HDA adduct, now by almost 21 kcal/mol. In experiment, only the DA adduct is observed. This may be explained by the HDA adduct undergoing a cycloreversion back to starting materials, which can undergo an essentially irreversible DA cycloaddition. However, we also located a transition structure corresponding to the [3,3]-sigmatropic rearrangement that provides an alternative pathway for the interconversion. The sigmatropic rearrangement of the HDA adduct is relatively facile in relation to the cycloaddition step, since this [3,3]-TS lies lower in energy than any of the cycloaddition TSs.

The geometries of the *endo* DA (**1**), *endo* HDA (**4**) and [3,3]-sigmatropic rearrangement (**6**) transition structures are rather similar, and lie within 2 kcal/mol in energy. The potential energy surface is very flat in the region of these structures. In the *endo* DA transition structure there is a C-O distance of 2.87 Å, which suggests that to some extent this structure can be considered as “bis-pericyclic”,<sup>9,12</sup> with intermolecular distances reflective of both DA and HDA bond-forming reactions. Intrinsic Reaction Coordinate (IRC) calculations were able to locate the energy minima that connect these transition structures, and no bifurcations were found on the energy surface. However, the relative positions of the cycloaddition and sigmatropic rearrangement transition states may well influence the periselectivity due to the shape of the potential energy surface and corresponding dynamical influences. The key transition structures are summarized in Figure 2.

The regioselectivity of an unsymmetrical diene (isoprene) was then investigated. Transition structures were located for the DA and HDA cycloaddition with 1-nitrocyclohexene. The *endo* transition structures are shown in Figure 3. The *exo* structures were located and all lie higher in energy than the corresponding *endo* structures (see Supporting Information). The HDA transition structures are found to be slightly favored kinetically, although thermodynamics favor the DA cycloadducts by over 19 kcal/mol.

[3,3]-Sigmatropic rearrangement transition structures were again located. These lie close in energy to the cycloaddition transition structures, as shown in Figure 4. Thus the sigmatropic rearrangement TS again presents an energetically accessible pathway for the HDA to interconvert to the DA adduct. Whereas the DA cycloadducts themselves are essentially isoenergetic, the transition structures leading to the *para*-substituted product are somewhat favored over their meta-substituted counterparts (DA:  $\Delta\Delta G^\ddagger$  0.6 kcal/mol, HDA:  $\Delta\Delta G^\ddagger$  0.9 kcal/mol, sigmatropic:  $\Delta\Delta G^\ddagger$  1.6 kcal/mol). Experimentally, the reaction of isoprene and nitrocyclohexene is unselective when performed in toluene, but in trifluoroethanol the *para*-substituted product dominates in a 15:1 ratio. Computed relative free energies of the regioisomeric pathways performed with implicit solvation reproduce this trend, as the  $\Delta\Delta G^\ddagger$  of DA and HDA pathways increase to 1.4 and 1.6 kcal/mol in favor of the *para*-substituted product. The M06-2X calculations predict that both direct DA and hetero-DA/sigmatropic rearrangement pathways are competitive, both forming the *para*-product.

Experimentally, the use of a hydroxylic solvent resulted in improved cycloaddition yields. A substantial increase in yield was observed with 2,2,2-trifluoroethanol as solvent, particularly under microwave conditions. The effects of solvation were evaluated computationally with an implicit continuum model and also using explicit molecules of 2,2,2-trifluoroethanol, as shown in Figure 5. The inclusion of a hydrogen-bonded trifluoroethanol molecule led to smaller activation barriers for HDA and sigmatropic rearrangement transition structures (we were unable to locate the DA transition structure), by around 4 kcal/mol. The thermodynamics of the Diels-Alder adduct and hetero-Diels-Alder adduct formation are changed only marginally by the inclusion of solvent. Therefore the effects of an alcoholic solvent are to enhance reaction rates for all pathways. Energetics computed with an implicit solvent model led to the same conclusions, with the barrier heights in close quantitative agreement with those with an explicit molecule of alcohol. The origins of this rate enhancement are due to the partial charge separation in the DA and HDA transition structures: the charges on the 1-nitrocyclohexene moiety are  $-0.18$  and  $-0.40$  in the DA and HDA structures, respectively. Specific hydrogen bonding interactions with the nitro group are strengthened, as the computed Mulliken charge on each of the two oxygen atoms increases from  $-0.40$  in the reactant to  $-0.45$  and  $-0.47$  in the DA and HDA transition structures, respectively.

### Conversion of Diels-Alder adducts of 1-nitrocyclohexene to the formal *trans*-Diels-Alder adducts of cyclohexene

Reductive hydrodenitration using tri-*n*-butyltin hydride in the presence of AIBN resulted in the formation of the denitrated *trans*-fused dehydrodecalin.<sup>1</sup> In the cycloaddition of 1-nitrocyclohexene to a range of dienes (2,3-dimethyl-1,3-butadiene, isoprene, 1,2-dimethylenecyclohexane and 2,3-diphenyl-1,3-butadiene) the initial *cis*-fused Diels-Alder stereochemistry can be converted to a *trans*-fused dehydrodecalin with 7-12:1 diastereoselectivity.<sup>1</sup>

We studied the stability and the interconversion of the tertiary carbon radicals formed in the radical denitration mechanism, and the irreversible hydrogen radical transfer from a trialkyltin hydride. The results are shown in Figure 6. Computations performed on the radical intermediates for the 2,3-dimethyl-1,3-butadiene/1-nitrocyclohexene Diels-Alder

cycloadduct show that the observed *trans* selectivity in the hydrodenitration is a consequence of the greater thermodynamic stability of the *trans*-fused bridgehead radical over the *cis* form. The tertiary radicals are appreciably pyramidal, but the interconversion via a planar transition state is calculated to be energetically feasible, and is able to occur much faster than the radical trapping with a trialkyltin hydride. Transition structures were located for hydrogen transfer from trimethyltin hydride to form *trans*- and *cis*-dehydrodecalins. Both transition structures have large distances between carbon and tin, and so the TS relative energies simply reflect the stability of each of the radical geometries. Whereas the *cis*-radical lies 2.6 kcal/mol above the *trans*-radical, the transition states differ in energy by 2.5 kcal/mol. The greater stability of the *trans*-radical and transition state is due to the absence of any axial substituents in the latter. The products of hydrogen abstraction differ by 3.2 kcal/mol, due to the same repulsive interactions in the *cis*-product. The same energetic trends are manifested in the UM06-2X energetics, with the *trans*-radical, TS and product favored over the corresponding *cis*-pathway by 1.4, 2.8 and 2.3 kcal/mol. By way of comparison, *trans*-decalin (decahydronaphthalene) is favored over its *cis*-stereoisomer by 2.5-3.1 kcal/mol. The dehydrodecalin cycloadducts lack a 1,3-steric interaction in the *cis*-isomer that is present for decalin, so the expected energy difference between *cis* and *trans* forms of dehydrodecalin is expected to be smaller than 2.5 kcal/mol. Calculated free energy differences between *cis* and *trans* pathways for the hydrodenitration of 1,2-diphenyl dehydrodecalin and 1-methyl dehydrodecalin are also in accord with the *trans*-selectivity of these systems (see Supporting Information).

The origins of the poor *trans*-selectivity in the hydrodenitration step when nitrocyclopentene was used experimentally were also investigated, as shown in Figure 7. Unlike the 6,6-bicyclic radical in Figure 6, the 5,6-bicyclic adduct formed from the cycloaddition of nitrocyclopentene is unable to adopt distinct *cis* and *trans* radical conformers after denitration. Therefore just a single radical conformer, planar about the radical carbon atom, results and this may react with trialkyltin hydride from either face. The UB3LYP relative free energies of the resulting two transition structures suggest these two pathways are isoenergetic, which is in accord with the low stereoselectivity of this process.

## Conclusions

The origins of regioselectivity and stereoselectivity in the *trans*-selective Diels-Alder/hydrodenitration sequence developed by Danishefsky have been determined with density functional calculations. In the cycloaddition between 1-nitrocyclohexene and a series of butadienes, the Diels-Alder adduct results from the Diels-Alder pathway but also by a hetero-Diels-Alder cycloaddition and subsequent [3,3]-sigmatropic rearrangement. The selectivity of the radical hydrodenitration step of 6,6-bicyclic adducts arises from the greater stability of the *trans*-decalyl radical intermediate and subsequent transition state involving hydrogen atom transfer.

## Supplementary Material

Refer to Web version on PubMed Central for supplementary material.

## Acknowledgments

This work was supported by NIH-GM36700 (K.N.H.), the Fulbright Commission, AstraZeneca and the Royal Commission for the Exhibition of 1851 (R.S.P). Computer time was provided in part by the UCLA Institute for Digital Research and Education (IDRE).

## References

1. Kim WH, Lee JH, Danishefsky SJ. *J Am Chem Soc.* 2009; 131:12576–12578. [PubMed: 19685875]
2. Denmark SE, Thorarensen A. *Chem Rev.* 1996; 96:137–165. [PubMed: 11848747]
3. Denmark SE, Kesler BS, Moon YC. *J Org Chem.* 1992; 57:4912–4924.
4. (a) Denmark SE, Cramer CJ, Sternberg JA. *Helv Chim Acta.* 1986; 69:1971–1989. (b) Denmark SE, Cramer CJ, Sternberg JA. *Tetrahedron Lett.* 1986; 27:3693–3696.
5. Denmark SE, Moon YC, Senanayake CBW. *J Am Chem Soc.* 1990; 112:311–315.
6. Denmark SE, Moon YC, Cramer CJ, Dappen MS, Senanayake CBW. *Tetrahedron.* 1990; 46:7373–7392.
7. Denmark SE, Dappen MS, Cramer CJ. *J Am Chem Soc.* 1986; 108:1306–1307.
8. Denmark SE, Stolle A, Dixon JA, Guagnano V. *J Am Chem Soc.* 1995; 117:2100–2101.
9. Çelebi-Ölçüm N, Ess DH, Aviyente V, Houk KN. *J Org Chem.* 2008; 73:7472–7480. [PubMed: 18781801]
10. Wade PA, Murray JK Jr, Shah-Patel S, Le HT. *Chem Commun.* 2002:1090–1091.
11. Gómez MV, Aranda AI, Moreno A, Cossío FP, de Cózar A, Díaz-Ortiz A, de la Hoz A, Prieto P. *Tetrahedron.* 2009; 65:5328–5336.
12. Doubleday C, Nendel M, Houk KN, Thweatt D, Page M. *J Am Chem Soc.* 1999; 121:4720–4721.
13. Doubleday C, Suhrada CP, Houk KN. *J Am Chem Soc.* 2006; 128:90–94. [PubMed: 16390135]
14. Kless A, Nendel M, Wilsey S, Houk KN. *J Am Chem Soc.* 1999; 121:4524–4525.
15. (a) Toma L, Romano S, Quadrelli P, Caramella P. *Tetrahedron Lett.* 2001; 42:5077–5080. (b) Caramella P, Quadrelli P, Toma L. *J Am Chem Soc.* 2002; 124:1130–1131. [PubMed: 11841256] (c) Quadrelli P, Romano S, Toma L, Caramella P. *Tetrahedron Lett.* 2002; 43:8785–8789. (d) Quadrelli P, Romano S, Toma L, Caramella P. *J Org Chem.* 2003; 68:6035–6038. [PubMed: 12868944]
16. Singleton DA, Hang C, Szymanski MJ, Meyer MP, Leach AG, Kuwata KT, Chen JS, Greer A, Foote CS, Houk KN. *J Am Chem Soc.* 2003; 125:1319–1328. [PubMed: 12553834]
17. Ess DH, Wheeler SE, Iafe RG, Xu L, Çelebi-Ölçüm N, Houk KN. *Angew Chem Int Ed.* 2008; 47:7592–7601.
18. Çelebi-Ölçüm N, Ess DH, Aviyente V, Houk KN. *J Am Chem Soc.* 2007; 129:4528–4529. [PubMed: 17385868]
19. Beno BR, Houk KN, Singleton DA. *J Am Chem Soc.* 1996; 118:9984–9985.
20. Khuong KS, Jones WH, Pryor WA, Houk KN. *J Am Chem Soc.* 2005; 127:1265–1277. [PubMed: 15669866]
21. Hayden AE, DeChancie J, George AH, Dai M, Yu M, Danishefsky SJ, Houk KN. *J Org Chem.* 2009; 74:6770–6776. [PubMed: 19663431]
22. Yoshikawa M, Okaichi Y, Cha BC, Kitagawa I. *Tetrahedron.* 1990; 46:7459–7470.
23. (a) Ono N, Miyake H, Kaji A. *J Chem Soc, Chem Commun.* 1982:33–34. (b) Ono N, Miyake H, Kaji A. *J Chem Soc, Perkin Trans 1.* 1987:1929–1935.
24. Guy A, Serva L. *Synlett.* 1994:647–648.
25. Frisch, MJ., et al. *Gaussian 09, revision A.02.* Gaussian, Inc; Wallingford, CT: 2009.
26. (a) Hayden AE, DeChancie J, George AH, Dai M, Yu M, Danishefsky SJ, Houk KN. *J Org Chem.* 2009; 74:6770–6776. [PubMed: 19663431] (b) Hayden AE, Paton RS, Becker J, Lim YH, Nicolaou KC, Houk KN. *J Org Chem.* 2010; 75:922–928. [PubMed: 20027998] (c) Spellmeyer DC, Houk KN. *J Org Chem.* 1987; 52:959–974. (d) Montgomery JA Jr, Frisch MJ, Ochterski JW, Peterson GA. *J Chem Phys.* 1999; 110:2822–2827. (e) Luft JAR, Winkler T, Kessabi FM, Houk KN. *J Org Chem.* 2008; 73:8175–8181. [PubMed: 18842059] (f) Leach AG, Wang R, Wohlhieter GE, Khan SI, Jung ME, Houk KN. *J Am Chem Soc.* 2003; 125:4271–4278. [PubMed: 12670249]
27. Zhao Y, Truhlar DG. *Theor Chem Acc.* 2008; 120:215–241.
28. Pieniazek SN, Clemente FR, Houk KN. *Angew Chem Int Ed.* 2008; 47:7746–7749.
29. Grimme S. *J Chem Phys.* 2006; 124:034108. [PubMed: 16438568]

30. (a) Barone V, Cossi M. *J Phys Chem A*. 1998; 102:1995–2001. (b) Cossi M, Rega N, Scalmani G, Barone V. *J Comput Chem*. 2003; 24:669–681. [PubMed: 12666158]
31. Takano Y, Houk KN. *J Chem Theory Comput*. 2005; 1:70–77.
32. Afeefy, HY.; Liebman, JF.; Stein, SE. Neutral Thermochemical Data. In: Linstrom, PJ.; Mallard, WG., editors. *NIST Chemistry WebBook*, NIST Standard Reference Database Number 69. National Institute of Standards and Technology; Gaithersburg MD: p. 20899<http://webbook.nist.gov>, (retrieved January 26, 2010)

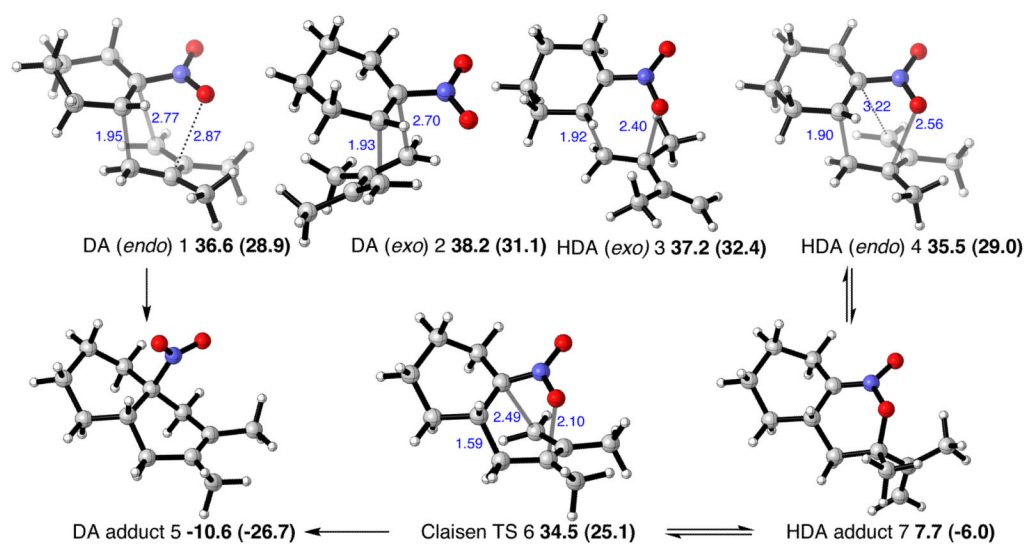


**Figure 1.** Transition structures and adducts for the cycloaddition of 2,3-dimethyl-1,3-butadiene and 1-nitrocyclohexene. Selected distances shown in Å, B3LYP/6-31G(d) relative free energies, with M06-2X/6-31G(d) in parentheses, shown in kcal/mol.



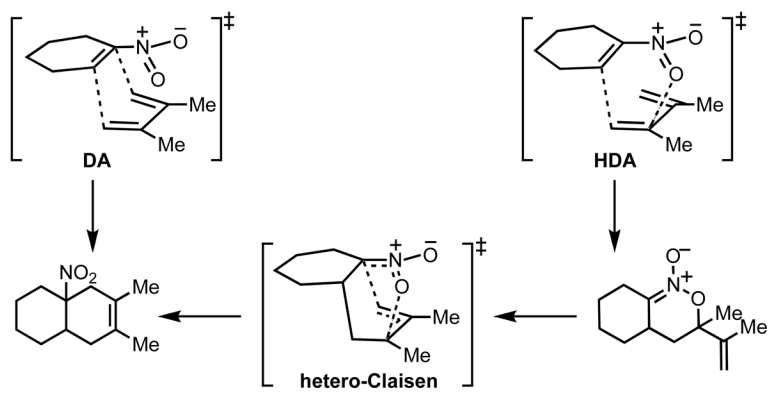


**Figure 2.** Summary of the low energy transition structures leading to the formation of the DA adduct.

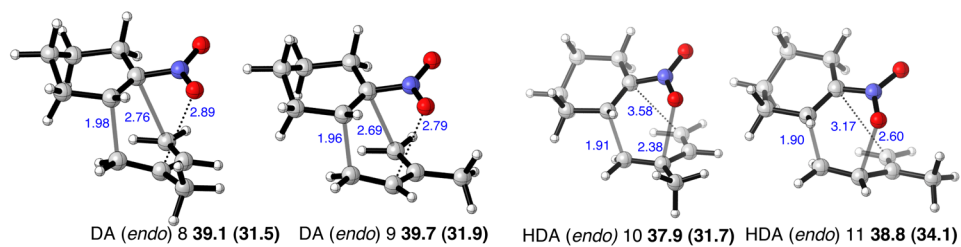


**Figure 3.** Transition structures for the cycloadditions of isoprene and 1-nitrocyclohexene. Selected distances shown in Å, B3LYP/6-31G(d) relative free energies, with M06-2X/6-31G(d) in parentheses, in kcal/mol.

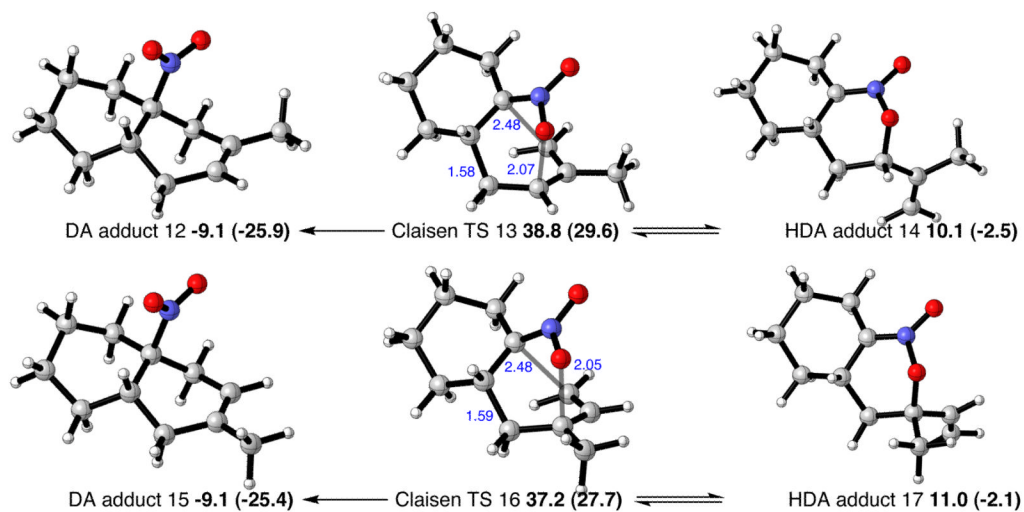


**Figure 4.** [3,3]-Sigmatropic rearrangement transition structures in the cycloaddition of isoprene and 1-nitrocyclohexene. Selected distances shown in Å, B3LYP/6-31G(d) relative free energies, with M06-2X/6-31G(d) in parentheses, in kcal/mol.

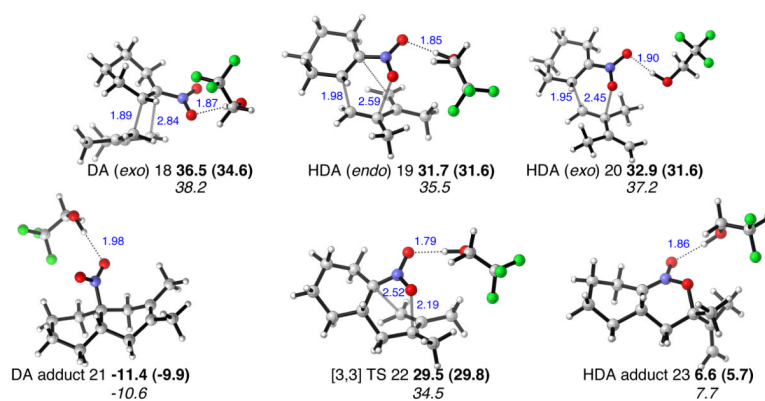


**Figure 5.** Solvent effects on the energetics of the cycloadditions of 1,3-butadiene and 1-nitrocyclohexene. Selected distances shown in Å, B3LYP/6-31G(d) relative free energies in kcal/mol, compared with implicit CPCM values in parentheses and gas-phase values in italics.

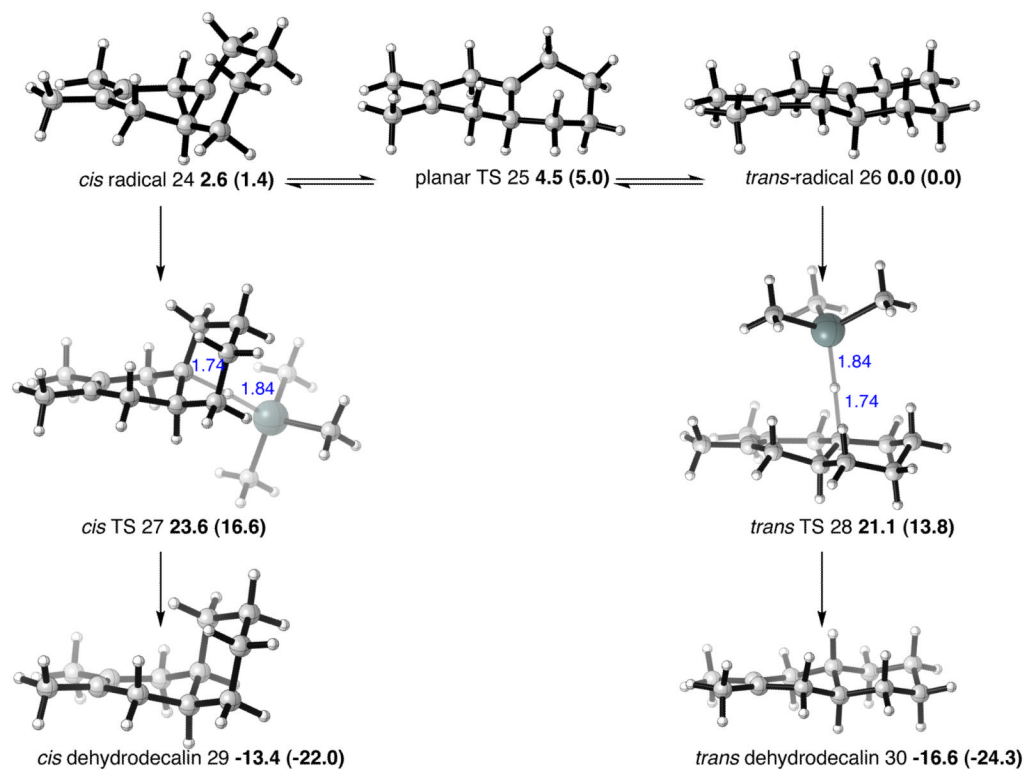


**Figure 6.** Bicyclic radicals and connecting transition structure, and hydrogen transfer TSs and dehydrodecalin products in the cycloaddition of 2,3-dimethyl-1,3-butadiene and 1-nitrocyclohexene. Selected distances shown in Å, UB3LYP/LANL2DZ relative free energies, UM06-2X/LANL2DZ in parentheses, in kcal/mol.

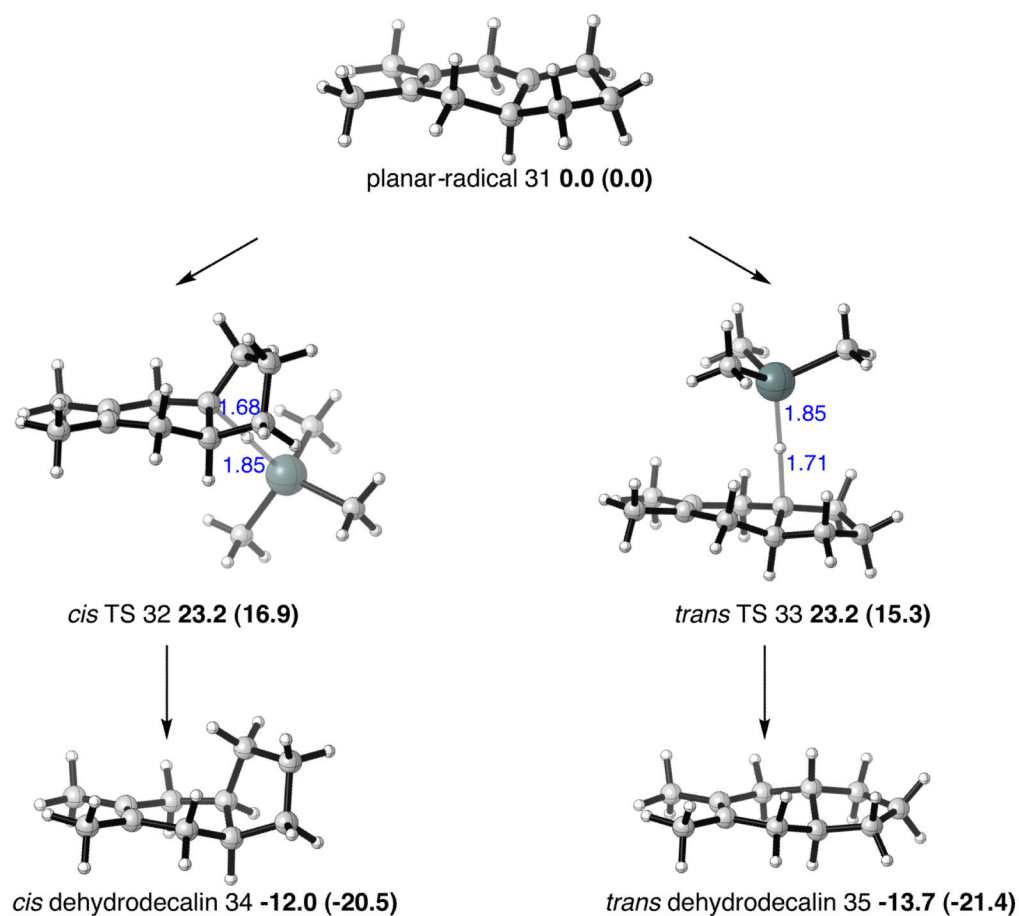
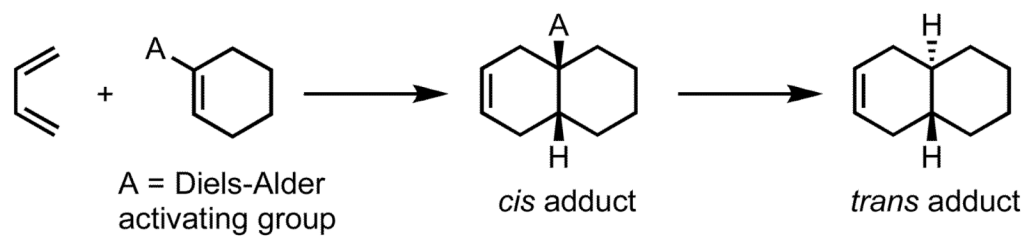
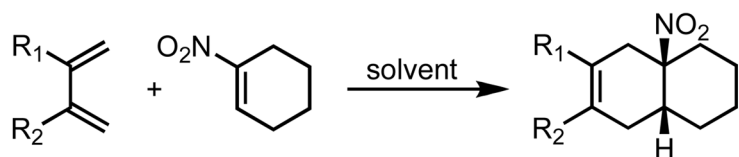


**Figure 7.** 6,5-Bicyclic radicals and connecting transition structure, and hydrogen transfer TSs and bicyclic products in the cycloaddition of 2,3-dimethyl-1,3-butadiene and 1-nitrocyclopentene. Selected distances shown in Å, UB3LYP/LANL2DZ relative free energies, UM06-2X/LANL2DZ in parentheses, in kcal/mol.



**Scheme 1.**  
The *trans* Diels-Alder paradigm involving a *cis*-dienophile.

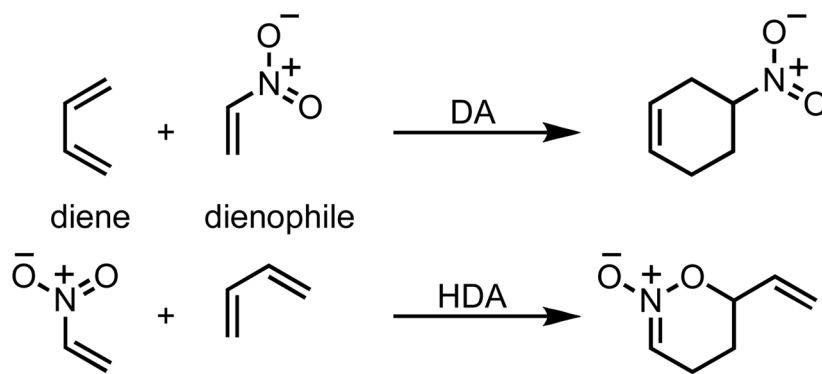


R <sub>1</sub> = R <sub>2</sub> = Me	toluene	140 °C, 36h	18%
R <sub>1</sub> = R <sub>2</sub> = Me	THF	130 °C, MW, 12h	17%
R <sub>1</sub> = R <sub>2</sub> = Me	EtOH	130 °C, MW, 14h	36%
R <sub>1</sub> = R <sub>2</sub> = Me	CF <sub>3</sub> CH <sub>2</sub> OH	130 °C, MW, 12h	78%
R <sub>1</sub> = H, R <sub>2</sub> = Me	CF <sub>3</sub> CH <sub>2</sub> OH	125 °C, MW, 14h	57%
R <sub>1</sub> = R <sub>2</sub> = (CH <sub>2</sub> ) <sub>4</sub>	CF <sub>3</sub> CH <sub>2</sub> OH	130 °C, MW, 10h	75%

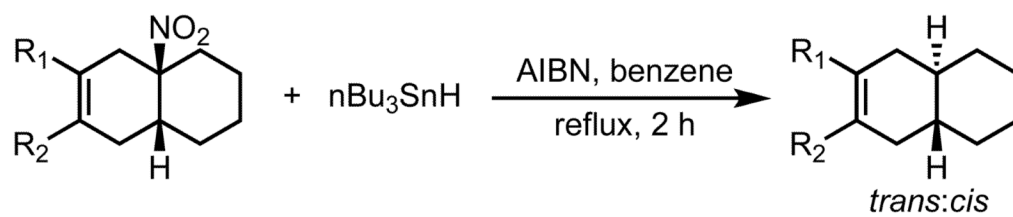
**Scheme 2.**

Cycloadditions of 1-nitrocyclohexene and hydrocarbon dienes. MW = microwave irradiation.





**Scheme 3.**  
Diels-Alder (DA) and hetero-Diels-Alder (HDA) cycloadditions of nitroalkenes.



$R_1 = R_2 = \text{Me}$	67%	8:1
$R_1 = \text{H}, R_2 = \text{Me}$	53%	8:1
$R_1 = R_2 = (\text{CH}_2)_4$	81%	12:1

**Scheme 4.**

Radical hydrodenitration of the DA adduct to yield *trans*-fused decalins.